ELSEVIER

Journal of Chromatography A, 777 (1997) 329–353

JOURNAL OF CHROMATOGRAPHY A

Principles and limitations of methods available for the determination of binding constants with affinity capillary electrophoresis

M.H.A. Busch*, J.C. Kraak, H. Poppe

Amsterdam Institute of Molecular Studies, Laboratory for Analytical Chemistry, University of Amsterdam, Nieuwe Achtergracht 166, 1018 WV Amsterdam, Netherlands

Received 13 November 1996; received in revised form 21 March 1997; accepted 3 April 1997

Abstract

At present there are five capillary zone electrophoresis (CZE) methods available for the measurement of binding (association) parameters viz. the frontal analysis method, the Hummel and Dreyer method, the affinity capillary electrophoresis, the vacancy peak and the vacancy affinity capillary electrophoresis methods. These methods exhibit their own advantages and limitations. In this paper the limitations of these five CZE methods will be explored with the aid of simulated concentration–position profiles of the interacting species. With the frontal analysis, the Hummel and Dreyer and the vacancy peak methods e.g., correct results for the binding parameters can only be obtained when the mobilities of e.g., a protein and the complex are equal. When the mobilities differ, the binding constants obtained with these methods will deviate systematically. The affinity capillary electrophoresis method on the other hand can only be performed when the mobility of the protein is not equal to the mobility of the complex. It is shown that this very necessary difference in the mobility between the free protein and the complex may lead to a deviation in the free ligand concentration and consequently in the binding constant. © 1997 Elsevier Science B.V.

Keywords: Affinity capillary electrophoresis; Binding studies; Frontal analysis; Hummel–Dreyer method; Vacancy peak method; Computer simulation; Association constants; Vacancy affinity capillary electrophoresis

1. Introduction

Various analytical techniques have been applied to determine the unbound (free) drug or the bound drug concentration in solution [1,2]. Capillary zone electrophoresis (CZE) already proved to be an attractive method to study binding interactions [3–26], but so far little attention has been given to the limitations of the available CZE methods. At present there are five CZE methods available to measure binding constants. With the exception of the vacancy affinity capillary electrophoresis (VACE) method these methods have been developed in high-performance liquid chromatography (HPLC) [1] before they were implemented in CZE, viz. the Hummel–Dreyer (HD) method, the affinity capillary electrophoresis (ACE) method, the frontal analysis (FA) method and the vacancy peak (VP) method. With the FA, the HD, the VP and the VACE methods the binding constant and the absolute numbers of the different binding sites can be determined. With the ACE method only the binding constant can be obtained [26]. The

*Corresponding author.

0021-9673/97/$17.00
PII S0021-9673(97)00368-3

principles of the CZE methods used for the determination of binding parameters are based on the separation of the interacting species, on the basis of their difference in mobility. The present study aims to explore the limitations of five CZE methods, with respect to the difference in the mobilities of the interacting species. A scheme will be outlined to guide the selection of an appropriate method for a system to be studied, taking into account their limitations and advantages.

2. Principles of the CZE methods

The migration of the zones in several CZE methods will be discussed in this section; viz. the FA, the HD, the VP, the ACE and the VACE methods.

The ACE method and the HD method have identical experimental set-ups. In both methods one of the interacting species is added to the buffer and the other one is injected. The methods differ in the choice of the parameter that is measured to obtain the binding constant. In the ACE method the change in the (average) mobility of the injected species, due to complex formation with the component present in the buffer, is used to calculate the binding constant. In the HD method the peak area of the vacancy peak of the component added to the buffer is used to obtain the binding constant.

The VACE and the VP methods have also identical experimental set-ups. In these two methods both interacting species are added to the buffer and neat buffer is injected. The concentration of one of these compounds is kept constant, while the concentration of the other one is varied. The VACE method differs only from the VP method in the choice of the parameter that is measured to obtain the binding constant. In the VACE method, the change in the mobilities of the species due to complex formation, present in the buffer, are used to calculate the binding constant. In the VP method the peak area of the vacancy peak of the component added to the buffer is used for that purpose.

The FA method uses a different experimental set-up. In this method the capillary is filled with neat buffer and a large plug of the sample, containing the interacting species, is injected.

In the following text we will, for the sake of simplicity, refer to the substances denoted as P (protein) and D (drug), forming a complex (C). Of course other substances than proteins and drugs can be electrophorized and their interaction studied with CZE. It is assumed that the complexation process is much faster than the migration process. That means, each molecule is converted many times during the migration. Its migration rate is a time-average i.e., an amount-average over the various forms. This is characterized with an average mobility $\mu_{A,B}$, indicating the average mobility of A in the presence of B.

Three cases A, B and C in which the mobility of D is smaller than the mobilities of the P and C will be discussed in detail. First the migration of the injected zones will be discussed for each method with the aid of a schematical illustration, after which the results of the full computer simulations will be presented. In case A the mobility of P is equal to the mobility of the complex (C), but larger than the mobility of D, $\mu_P=\mu_C>\mu_D$, in case B it is assumed that the mobility of the complex (C) is larger than the mobility of P, which is assumed to be larger than the mobility of D; $\mu_C>\mu_P>\mu_D$, and in case C it is assumed that the mobility of the complex (C) is smaller than the mobility of P, which is assumed to be larger than the mobility of D; $\mu_C<\mu_P>\mu_D$.

In case D, E and F the mobility of D is always larger than the mobilities of P and D ($\mu_D>\mu_P$, μ_C), contrary to case A, B and C where the mobility of D was always smaller than the mobility of P and C ($\mu_D<\mu_P$, μ_C). When comparing the mobility of P and C case D is analogous to case A, case E is analogous to case B and case F is analogous to case C:

		$\mu_D>\mu_P$, μ_C		
		D	E	F
	A	$\mu_C=\mu_P$		
$\mu_D<\mu_P$, μ_C	B		$\mu_C>\mu_P$	
	C			$\mu_C<\mu_P$

In case D the mobility of P is equal to the mobility of the complex (C), but smaller than the mobility of D, $\mu_D>\mu_P=\mu_C$, in case E it is assumed that the mobility of the drug is larger than the mobility of the

complex (C) which in turn is assumed to be larger than the mobility of P, $\mu_D > \mu_P < \mu_C$, and in case F it is assumed that the mobility of the drug is larger than the mobility of the protein (P) which in turn is assumed to be larger than the mobility of the complex (C) $\mu_D > \mu_P > \mu_C$.

The descriptions are valid for species forming a 1:1 complex, the case of multiple equilibria (formation of two or more complexes) will be discussed separately.

The principles of these five CZE methods have already been described in detail [27], and will therefore be mentioned only briefly in the present work. For a practical comparison of the applicability of these five methods we refer to a previous paper [27].

This paper will be focused on the migration processes of the above mentioned CZE methods.

2.1. Computer simulations

The described migration processes were simulated with a computer program written in Turbo Pascal, version 7.0 (Borland, Scotts Valley, CA, USA). The algorithm involved 8000 sections of the capillary. In each iteration step the equilibrium in each slice was calculated with a Newton–Raphson algorithm, solving the equation:

$$[P_{total}] = [P_f]\frac{K_b[D_{total}]}{(1 + K_b[P_f])} \quad (1)$$

which can be derived from the two mass balances:

$$[P_{total}] = [P_f] + [C]; \quad [D_{total}] = [D_f] + [C] \quad (2)$$

and the equilibrium relation:

$$[C] = K_b[D_f] \cdot [P_f] \quad (3)$$

where $[P_{total}]$ and $[D_{total}]$ are the total concentrations of P and D, respectively, $[P_f]$ and $[D_f]$ are the free concentrations of P and D, respectively, [C] is the concentration of the formed complex and K_b is the binding constant. In the equation, after each transport step the total concentrations of P and D, $[P_{total}]$ and $[D_{total}]$, respectively are known. Once $[P_f]$ is found by simple substitution one finds $[D_f]$ and [C]. Migration fluxes in the field E were then found (in terms of total amounts) by:

$$J_P = E(\mu_C[C] + \mu_P[P_f]);$$
$$J_D = E(\mu_C[C] + \mu_D[D_f]) \quad (4)$$

With a chosen time increment Δt and a chosen space increment Δz the finds change in the total concentration of P in section n:

$$\Delta[P^n_{total}] = \frac{\Delta t}{2\Delta z}\left(J_P^{n-1} - J_P^{n+1}\right) \quad (5)$$

where unit ratio of cross section and volume of the capillary section has been assumed, as we are interested only in relative results, and $n-1$, n and $n+1$ refer to the section number.

The change in $[D_{total}]$ was calculated in the same way.

This algorithm generates negative concentrations and leads to instabilities, as has been discussed at length in many publications (see e.g., Refs. [28,29]). A diffusion term has to be added. This had the form:

$$\Delta[P^n_{total}] = \frac{\Delta t}{\Delta z}\left([P^{n-1}_{total}] - 2[P^n_{total}] + [P^{n+1}_{total}]\right) \quad (6)$$

which is obtained when the diffusion coefficient is set to a value such that $D/(\Delta z)^2$ equals 1. Again, this could be done for the same reason as given above.

Values of Δt and E were chosen to obtain maximum simulation speed while avoiding negative concentrations. After each step new values for $[P_{total}]$ and $[D_{total}]$ were available and a new equilibrium step could be applied. The simple procedure yields unreliable results with respect to dispersion [30]. However, these were not relevant in this study and their disturbing effect was kept small by simply taking many sections (8000). Injection was simulated by inserting the injection composition in a bunch of slices of about 3200 for the FA and 200 for the HD (ACE) and the VP (VACE) methods.

In the discussed simulations of cases A, B and C the mobility of D was arbitrarily set to $20 \cdot 10^{-9}$ $m^2/V\,s$, smaller than the mobility of P and C. In cases D, E and F the mobility of D was set to $80 \cdot 10^{-9}$ $m^2/V\,s$, larger than the mobility of P and D.

Furthermore in cases A and D, it was assumed that the mobilities of P, μ_P, and the mobility of the complex, μ_C, were equal: arbitrarily they were set to $50 \cdot 10^{-9}$ $m^2/V\,s$.

In cases B and E the mobility of P was again set to

$50 \cdot 10^{-9}$ m^2/V s, but the mobility of the complex was set to $70 \cdot 10^{-9}$ m^2/V s.

In cases C and F the mobility of P was again set to $50 \cdot 10^{-9}$ m^2/V s, but the mobility of the complex was set to $30 \cdot 10^{-9}$ m^2/V s.

The binding constant was set to $1.60 \cdot 10^4$ l/mol in all experiments. In the HD (ACE) experiments the concentration of D in the buffer, $[D_{buffer}]$, was set to 100 μmol/l. In the VP (VACE) and the FA experiments the total concentrations of P and D, $[P_{total}]$ and $[D_{total}]$, respectively were set to 100 μmol/l.

The concentration–position profiles of P_f, D_f and C, are shown separately. For cases A, B and C the simulated concentration–position profiles are shown for two points of time (1 and 2) in the capillary, for cases D, E and F only for one point of time (2). The (total) electropherogram should be seen as the sum of these separate concentration–position profiles.

2.2. Hummel and Dreyer (HD) method

In the HD method the capillary is filled with buffer containing D in varying concentrations, and a fixed amount of P is injected into the capillary. A typical elution profile is schematically shown in Fig. 1A.

A positive peak appears corresponding to the P–D complex, indicated by (●), and a negative one emerging at the migration time of D, indicated by (*). The area of the negative peak is directly related to the amount of D bound to P, $[D_b]$. This amount of bound D may be quantitated from external or internal calibration [27,31,32]. The value of the free D concentration, $[D_f]$, also needed for the evaluation of the equilibrium, is assumed to be equal to the concentration of D in the buffer [32].

2.2.1. Case A: $\mu_C = \mu_P > \mu_D$

In Fig. 2a (lines 1–5) the migration process is illustrated for the case where a small amount of P is injected into the buffer containing D.

The migration process in a HD experiment may be described in the following manner: after injection (line 1) P will form a complex with D, present in the buffer, while migrating through the buffer (line 2). As a result, molecules of D will be consumed by P, to form complex (C), causing a vacancy in the concentration of D in the buffer (line 2). After a short time a steady state will be reached (line 3) according to the equilibrium and the concentration of D in the buffer; the number of bound molecules of D per molecule of P is fixed by the concentration of D in the buffer and therefore can be considered constant during elution [32]. The local free D concentration will be equal to that in the buffer, when the mobilities of free P and the complex are equal.

For deriving the relations between the concentrations involved one has to use the moving boundary equations [33]. When applied for substance D,

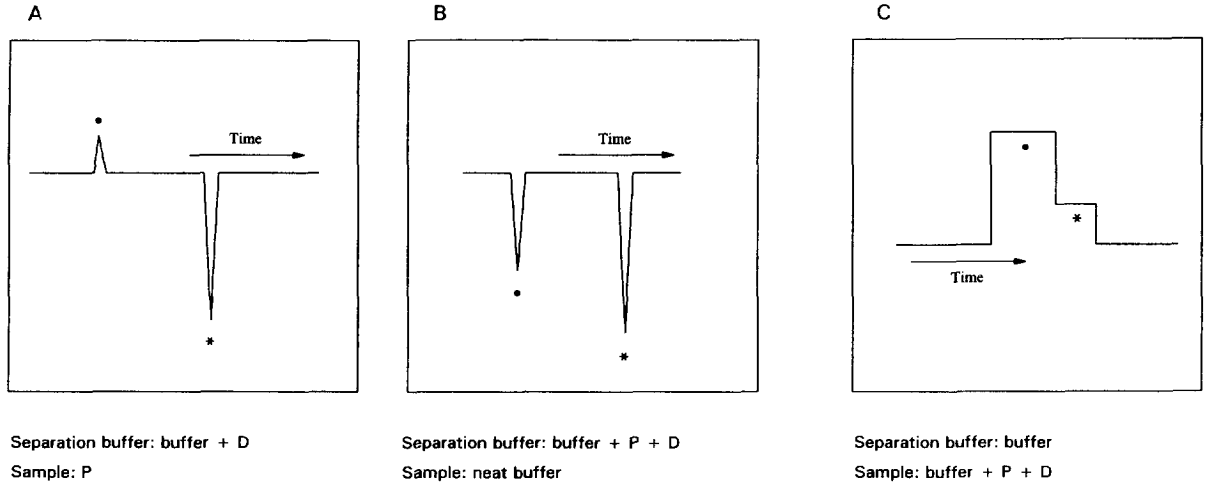

Fig. 1. Schematic elution profiles of the methods. (A) HD (ACE); (B) VP (VACE); (C) FA.

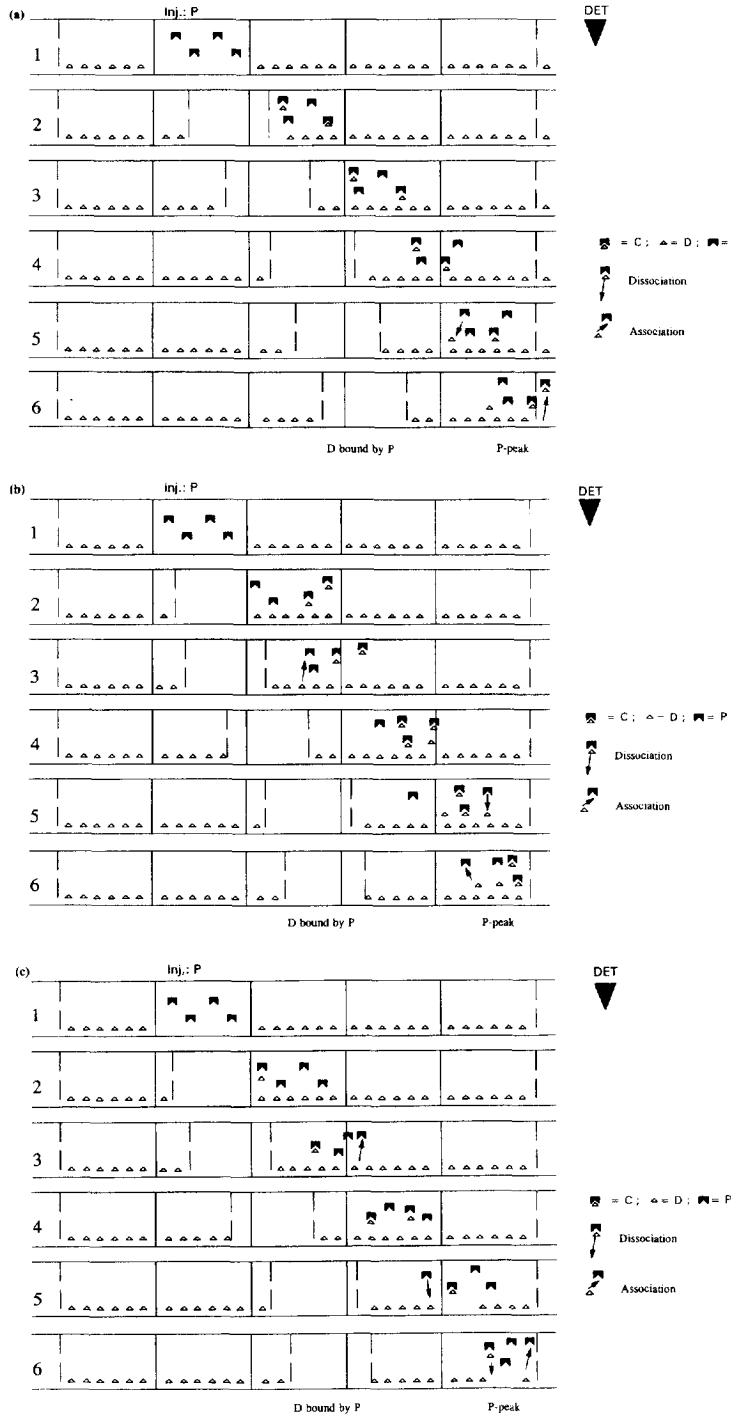

Fig. 2. (a) Illustration of the migration of the injection zone in the HD (ACE) method for case A; assumption: $\mu_C = \mu_P > \mu_D$. (b) Illustration of the migration of the injection zone in the HD (ACE) method case B; assumption: $\mu_C > \mu_P > \mu_D$. (c) Illustration of the migration of the injection zone in the HD (ACE) method case C; assumption: $\mu_C < \mu_P > \mu_D$.

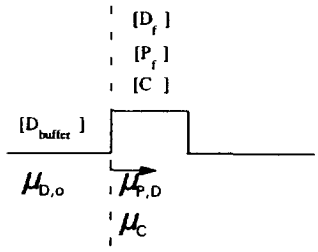

Fig. 3. Illustration of the moving boundary equation.

and for one of the boundaries of the P zone, it is (see Fig. 3):

$$[D_{buffer}](\mu_D - \mu_{P,D}) = [D_f](\mu_D - \mu_{P,D}) + [C](\mu_C - \mu_{P,D}) \quad (7)$$

where μ_D, $\mu_{P,D}$ and μ_C represent, respectively the mobility of the free D, the average mobility of P in the presence of D and the mobility of the complex, C.

This equation, as explained in Ref. [33] and numerous books (e.g., Ref. [34]), must hold when the boundary is to be stable, i.e., not resolve into two or more boundaries. Briefly it says that, in a coordinate system moving with the velocity of the zone, here $\mu_{P,D}$ times the field strength, the amounts carried to the boundary from the left must equal those carried away to the right.

Eq. (7) simplifies for $\mu_P = \mu_C$, because then the movement of P is independent of its form and $\mu_{P,D} = \mu_P = \mu_C$. In that case the term with [C] in the Eq. (7) cancels, and one finds $[D_f] = [D_{buffer}]$. As an additional result the peak has a symmetrical shape. This fact is interesting and allows for simple, reliable data handling.

2.2.2. Case B: $\mu_C > \mu_P > \mu_D$

The migration process for case B is illustrated in Fig. 2b, and may be described as follows: after injection, P starts forming a complex with D present in the buffer again (line 1 and 2).

As soon as the complex is formed it migrates to the front edge of the zone of P (line 3) because now $\mu_C > \mu_P$, leaving a gap in the concentration of C at the rear end of the zone.

To retain equilibrium there, *more* molecules of D will be consumed by free P (line 3). This results in a larger negative peak (line 4), when compared to case A. After a short time, a steady state will be reached with two separate zones: one of P and one being a vacancy in D. While migrating, at the front edge of the P-zone, complex is "moving out of the zone" and will dissociate to retain equilibrium, resulting in free P and free D (line 5). The formed free D will migrate with its own mobility, μ_D, "left behind" by the complex and free P. In the P-zone the $[D_f]$ concentration is higher than the concentration added to the buffer $[D_{buffer}]$. This represents the counterpart of the enlargement of the vacancy (mass balance). At the rear edge of the P-zone, P, migrating slower than the complex, but faster than the free D, will catch up with free D produced by dissociation of the complex at the front edge of the zone (line 6). Therefore the increase of $[D_f]$ in the zone will migrate with the average mobility of P. The value calculated for the amount of D bound, $[D_b]$, will be too high in case B. As a result the obtained binding parameters with the HD method will contain a systematic error and will also be too high. The extent of the effect depends on the difference in the mobilities of free P and the complex.

Another way to derive this is considering the moving boundary Eq. (7), showing that $[D_f]$ cannot be equal to $[D_{buffer}]$ when $\mu_C \neq \mu_{P,D}$. The vacancy in D is larger for ($\mu_C > \mu_P$) than for case A ($\mu_C = \mu_P$), as a result of the additional consumption mentioned above.

2.2.3. Case C: $\mu_C < \mu_P > \mu_D$

The migration process for case C is illustrated in Fig. 2c, and may be described as follows: after injection, P starts forming a complex with D present in the buffer again (line 1 and 2). Free P will migrate to the front edge of the zone (line 3) because now $\mu_P > \mu_C$, leaving a gap in the concentration of P at the rear end of the zone.

To retain equilibrium there, *less* molecules of D will be consumed by free P (line 3). This results in a smaller negative peak (line 4), when compared to case A. After a short time, a steady state will be reached with two separate zones: one of P and one

being a vacancy in D. The value calculated for the amount of D bound, $[D_b]$, will be too low. The obtained binding parameters with the HD method will contain a systematic error and will also be too low. The extent of the effect depends on the difference in the mobilities of free P and the complex.

While migrating, at the front edge of the P-zone, free P is "moving out of the zone" and will associate with D to retain equilibrium, resulting in complex (line 5). In the P-zone the $[D_f]$ concentration is lower than the concentration added to the buffer $[D_{buffer}]$. Another way to derive this is considering the moving boundary Eq. (7), showing that $[D_f]$ cannot be equal to $[D_{buffer}]$ when $\mu_C \neq \mu_{P,D}$.

2.3. Simulated concentration–position profiles for the HD and the ACE methods

2.3.1. Case A: $\mu_C = \mu_P > \mu_D$

The simulated concentration–position profiles for the HD method for case A are shown in Fig. 4A. When the mobilities of free P and the complex are equal a positive peak in the profiles of the complex and free P appears, representing respectively, the formed complex and free P. Both are migrating with the same mobility. The profile of free D shows only one negative peak as expected. migrating with the mobility of the free drug. The area of this negative peak can be related to the bound concentration of D.

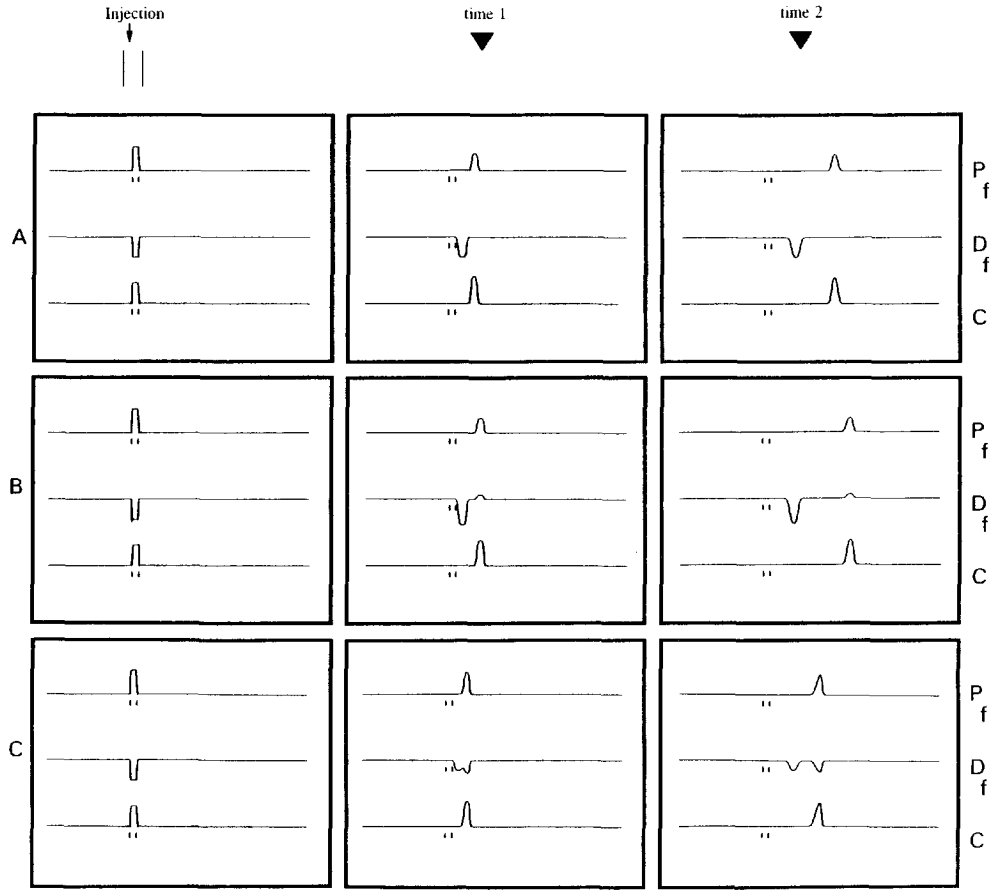

Fig. 4. Simulated concentration–position profiles for the HD (ACE) method, abscissa is position (1 and 2) in capillary. Injection marked by (| |). Assumptions: (A) $\mu_C = \mu_P > \mu_D$; (B) $\mu_C > \mu_P > \mu_D$; (C) $\mu_C < \mu_P > \mu_D$.

As can be seen in the migration profile of free D, the concentration of free D in the free P and complex zone is equal to the concentration of D in the buffer, it is therefore correct to assume that the equilibrium is measured at the $[D_{buffer}]$ value.

2.3.2. Case B: $\mu_C > \mu_P > \mu_D$

In Fig. 4B the simulated concentration–position profiles are shown when the mobility of free P is smaller than the mobility of the complex. In case B the profile of free D shows again a negative but in addition a positive peak at the position of P. The area of the negative peak is enlarged by a corresponding amount (mass balance) and does no longer accurately reflect the amount of bound D. Indeed, it can be seen that the area of the negative peak in case B is larger than the area of the negative peak in case A. This will result in a value for the amount of bound D, which is too high. Within the migrating zone of P the concentration of free D is higher than in the buffer, because extra D was consumed before the steady state was reached.

The deviation of the concentration of D within the P-zone leads to deformation and broadening of that zone, as can be seen in the simulations (Fig. 4B, line D_f, P_f and C). This is to be expected, as the average velocity of P becomes a function of its own concentration, via its influence on the $[D_f]$ value. In other words, the degree of complexation of P, and with that its $\mu_{P,D}$ value, changes with its own concentration. Therefore the zone must develop a sharp and a diffuse boundary. In case B ($\mu_C > \mu_P$) the diffuse boundary is at the rear, because $\mu_{P,D}([P]=0)$ is smaller than $\mu_{P,D}([P]\neq 0)$.

2.3.3. Case C: $\mu_C < \mu_P > \mu_D$

In Fig. 4C the simulated concentration–position profiles are shown when the mobility of free P is larger than the mobility of the complex. In this case the profile of free D shows two negative peaks. As can be seen the area of the D-vacancy in case C is smaller than the area of the D-vacancy in case A. This will result in a value for the concentration of bound D, $[D_b]$, that is too low in case C.

The second negative peak (first one to be detected) in the elution profile of free D migrates with the mobility of P. Locally, in the migrating zone of P, the concentration of free D is lower than in the buffer, because D will be consumed during the migration process by free P that is migrating "out" of the P-zone to retain equilibrium.

As can be seen when comparing Fig. 4A and Fig. 4C, the peaks of free P and the complex, are also somewhat broader in case C than in case A. This is caused by the mobility difference between free P and the complex.

In Table 1 an overview is presented of the deviation of the values of K_b using the HD method under the conditions chosen.

2.4. Affinity capillary electrophoresis (ACE) method

As mentioned before, the experimental set-up of the ACE method and the HD method are identical. Also in the ACE method one component is added in varying concentrations to the buffer, and the other one is injected (Fig. 1A). The concentration of the injected component is fixed. For instance D is added to the buffer and P is injected. In the ACE method the mobility of P as a function of the concentration of D in the buffer is monitored [35,36]. The peak of P shifts upon increasing the concentration of D in the buffer. The average mobility is determined by the fraction P free, α, migrating with the mobility of free P, $\mu_{P,o}$, and the fraction P bound $(1-\alpha)$, migrating with the mobility of the complex, μ_C, of the (injected) amount of P. The average mobility of the peak of P, $\mu_{P,D}$, can be expressed in the following way:

$$\mu_{P,D} = (1-\alpha)\mu_C + \alpha\mu_{P,o} \quad (8)$$

The ACE method, relates the change in the mobility $\mu_{P,D}$ of P, present in the sample, to the

Table 1
Predicted deviation of the binding constant (K_b) for the HD, the VP and the FA methods for cases A, B, C, D, E and F

	HD method	VP method	FA method
Case A	Correct	↑	Correct
Case B	↑	↑	↓
Case C	↓	↓	↑
Case D	Correct	↑	Correct
Case E	↓	↓	↑
Case F	↑	↑	↓

concentration of D present in the buffer, $[D_{buffer}]$. This enables the determination of the binding constant K_b [35].

Because the experimental set-up of the ACE method is identical to the HD method the described elution processes (Fig. 2a–c) and the results of the computer simulations (Fig. 4A–C) obtained for the HD method are also valid for the ACE method.

Therefore only the results of the computer simulations on the binding constant will be discussed. These are presented in Table 2.

2.4.1. Case A: $\mu_C = \mu_P > \mu_D$

The concentration of free D in the zone of migrating P is equal to the concentration of D in the buffer in case A, as was already discussed with the HD method (Fig. 4A).

Although the ratio of the fractions free and bound P, $[P_f]/[P_b] = (\alpha)/(1-\alpha)$, is shifted towards the fraction bound P upon increasing the concentration of D in the buffer, this will not be reflected in the mobility of the peak of P, since μ_C is equal to $\mu_{P,o}$. The ACE method can therefore not be used in case A.

2.4.2. Case B: $\mu_C > \mu_P > \mu_D$

If the mobility of free P is not equal to the mobility of the complex, a shift in the mobility of the peak of P will be observed upon increasing the concentration of D in the buffer. As a result the ACE method can be used in case B to obtain the binding constant. The shift in the mobility of P is reflecting the shift in the ratio of free and bound P. However, as already discussed with the Hummel–Dreyer method (Fig. 4B), the concentration of free D in the migrating zone of P is higher than the concentration of D in the buffer in case B. As a result of the elevated free D concentration in the migrating zone of P, more complex will be formed in case B when compared with case A. This will result in a larger shift in the mobility of the peak of P than would be the case if the concentration of free D in the migrating zone of P would be equal to the concentration D in the buffer. With the ACE method a binding curve is constructed by plotting the (average) mobility of the peak of P versus the concentration of D in the buffer. In case B this plot will result in a systematic error in the estimation of the binding constant, because the local concentration of free D in the migrating zone of P, $[D_f]$, is not equal to the concentration of D in the buffer, $[D_{buffer}]$. As a result, the values estimated for the binding constant, K_b will be too high when $\mu_C > \mu_P$. The value obtained for K_b with the aid of our computer simulations was 9% too high for the conditions chosen (see Table 2).

Table 2
Values for K_b obtained for the ACE method for cases A, B, C, D, E and F using computer simulations

	P-peak, $K_b \cdot 10^4$ l/mol
Case A	Impossible
Case B	1.74 (+9%)
Case C	1.04 (−35%)
Case D	Impossible
Case E	0.87 (−45%)
Case F	2.11 (+32%)

K_b theoretical: $1.60 \cdot 10^4$ l/mol, $[P_{sample}]$: 50 μmol/l and $[D_{buffer}]$: 0–2000 μmol/l.

2.4.3. Case C: $\mu_C < \mu_P > \mu_D$

The ACE method can also be performed in case C. However, as already discussed with the HD method (Fig. 4C), in case C the concentration of free D in the migrating zone of P is lower than the concentration of D in the buffer. As a result of the decreased free D concentration in the migrating zone of P, less complex will be formed in case C when compared with case A. This will result in a smaller shift in the mobility of the peak of P than would be the case if the concentration of free D in the migrating zone of P would be equal to the concentration D in the buffer. The binding constant obtained in case C will therefore contain a systematic error: the values estimated for the binding constant with the aid of computer simulations for K_b were 35% too low in case C for the chosen conditions (see Table 2).

2.5. Vacancy peak (VP) method

In the vacancy peak (VP) method, the capillary is filled with buffer containing both P and D. The concentration of one of the components is fixed and the concentration of the other component is varied

[27,37,38]. The situation will be discussed in which the concentration of P is kept constant. A small volume of neat buffer is injected into the capillary and the power supply is switched on.

Two negative peaks will appear in the electropherogram (Fig. 1B). The first (negative) peak is detected because in this zone free P and the complex are lacking, indicated by (●). The second (negative) peak is detected because in this zone free D is lacking, indicated by (*). The area of the first peak will reflect the concentration of free P and complex in the buffer and the second peak will reflect the concentration of free D in the buffer [37].

2.5.1. Case A: $\mu_C = \mu_P > \mu_D$

The migration process of case A is shown in Fig. 5a (lines 1–5). The occurrence of the two negative peaks (vacancies) may be described in the following manner: At the rear edge of the plug (Fig. 5a, line 1–2), free P and C are migrating faster into the injection zone then D, leaving D behind, and finally catching up with free D from the front edge of the injection zone. Because the average mobility of free P is the same throughout the system a single vacancy will be preserved (line 3). In this vacancy, the D-concentration equals the original value. A vacancy in D develops simultaneously.

After a certain time, the zone lacking of free P and C and the zone lacking of D will be separated by a zone in which the equilibrium is attained again (line 4). From that point on a steady state is reached, resulting in two negative peaks in the electropherogram.

In the D vacancy, part of the complex will dissociate to retain the equilibrium, generating free P and free D (line 5) there. The free D concentration in this zone will therefore not be equal to the concentration of free D in the buffer.

2.5.2. Case B: $\mu_C > \mu_P > \mu_D$

The migration process of case B is shown in Fig. 5b (lines 1–5). A similar reasoning may be applied here for the occurrence of the negative peaks (lines 1–3).

In case B however, the complex is migrating faster (line 3) into the zone lacking of D, than free P and will dissociate to retain the equilibrium (line 4). Therefore, in case B, relatively more complex will migrate into this zone and dissociate before the steady state will be reached. The generated free D will migrate with its own mobility, left behind by the free P (line 4); free P will start migrating towards the front edge of the zone. At the rear edge free P that is entering the zone will catch up (line 4–5) and associate with the free D migrating ahead (liberated by dissociation of C). As a result, the relative complex concentration in this zone will be higher when compared with case A. The dissociation of the extra amount of complex in this zone will liberate more free P and free D when compared to case A. Therefore the area of the peak representing the concentration of free D in the buffer will be smaller in case B when compared to case A.

The first negative peak to be detected is representing a vacancy in the concentration of the complex and free P. At the front edge of the zone caused by a vacancy in (total) P relatively more P will be present (line 4), as a result of the difference in the mobilities between free P and the complex. Free D will be consumed by free P at the front edge of the zone to retain the equilibrium (line 4), causing a vacancy in the local free D concentration. At the rear edge of this zone complex will migrate into this vacancy and will dissociate because P (and also D) are lacking here. As a result of the difference in mobility, the zone of free P and the complex may be broadened, when compared to case A.

2.5.3. Case C: $\mu_C < \mu_P > \mu_D$

The migration process of case C is shown in Fig. 5c (lines 1–5). A similar reasoning as discussed for case A may be applied here for the occurrence of the negative peaks (lines 1–3). In case C however, P is migrating faster (line 3) into the zone lacking of D, than C. At the rear edge of the zone complex will dissociate because D is lacking there (line 3). The area of the negative peak in the elution profile of free D is larger when compared to case A, because in case C no free D is liberated in this vacancy by dissociation of the complex. The area of the negative peak in the elution profile of the free D in case C will approximate the free D concentration in the buffer the best.

The first negative peak to be detected is representing a vacancy in the concentration of the complex and free P. At the front edge of the P-vacancy

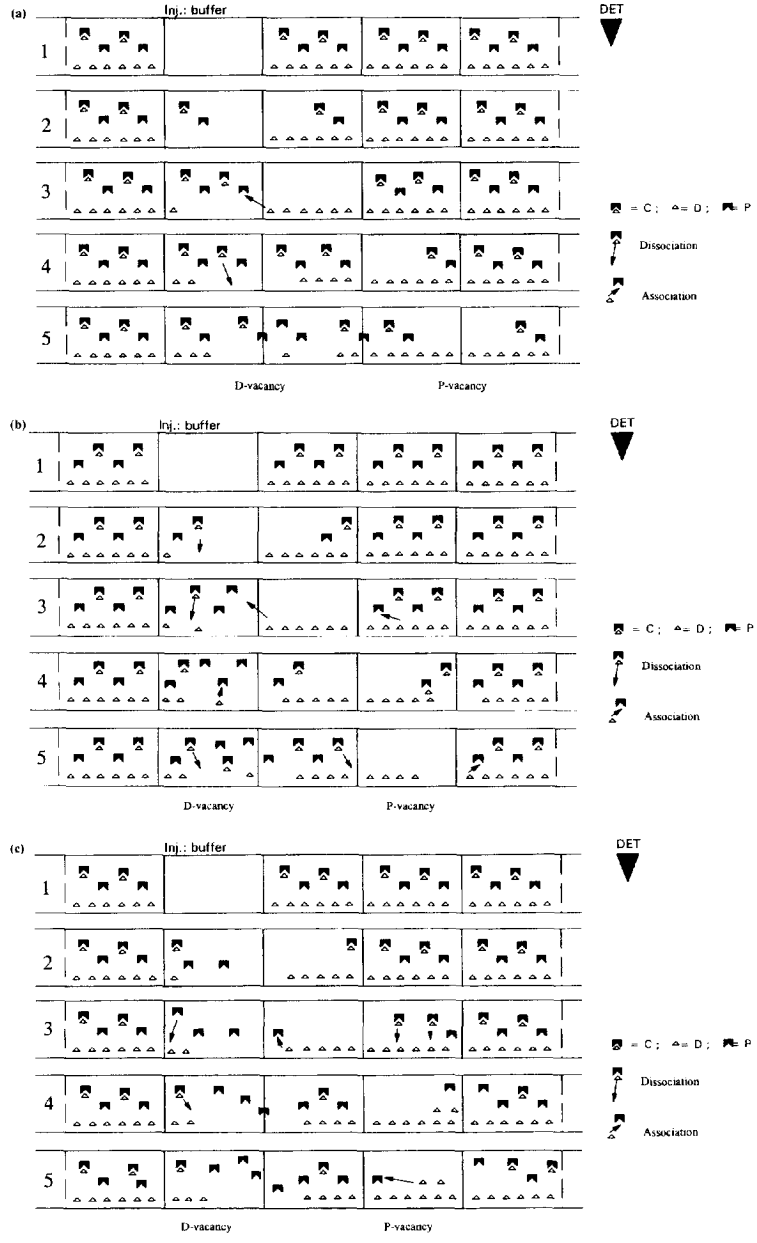

Fig. 5. (a) Illustration of the migration of the injection zone in the VP (VACE) method for case A; assumption: $\mu_C = \mu_P > \mu_D$. (b) Illustration of the migration of the injection zone in the VP (VACE) method for case B; assumption: $\mu_C > \mu_P > \mu_D$. (c) Illustration of the migration of the injection zone in the VP (VACE) method for case C; assumption: $\mu_C < \mu_P > \mu_D$.

relatively more complex will be present (line 3), because P is migrating faster. Complex will dissociate there to retain equilibrium (line 3–4), liberating free D. As a result the local free D concentration will be increased in the P-vacancy.

At the rear edge of the zone P will migrate "into" this vacancy and associate with the (liberated) free D to form complex. As a result of the difference in mobility, the zone of free P and the complex may be broadened (asymmetric), when compared to case A.

2.6. Simulated concentration–position profiles for the VP and the VACE methods

2.6.1. Case A: $\mu_C = \mu_P > \mu_D$

The simulated concentration–position profiles for case A are shown in Fig. 6A. Only one negative peak can be seen in the profile of free D. The area of this negative peak "represents" the concentration of free D in the buffer. However in case A the area representing the concentration free D in the profile of D will not reflect the "true" free D concentration in the buffer because also free D is generated by the dissociation of the complex. The area will be too small, suggesting that more D was bound by P than is really the case. As a result the values found for the binding parameters will be too high. The electropherogram, observed with e.g., UV, is a summation of the separate concentration–position profiles: the area of the negative peak in the profile of the complex is more or less equal to the positive peak in the profile of free P. When the absorbtivities of free P and C are equal these areas will not affect the area of the D-vacancy in the resulting electropherogram.

In the profile of the complex two negative peaks can be seen. The largest one is migrating with the mobility of the complex, representing the complex concentration in the buffer. The second one (smallest) is arising at the migration time of D. In the zone lacking of free D, part of the complex will dissociate and therefore a negative peak in the profile of the complex will arise in this zone and a corresponding positive peak in free P.

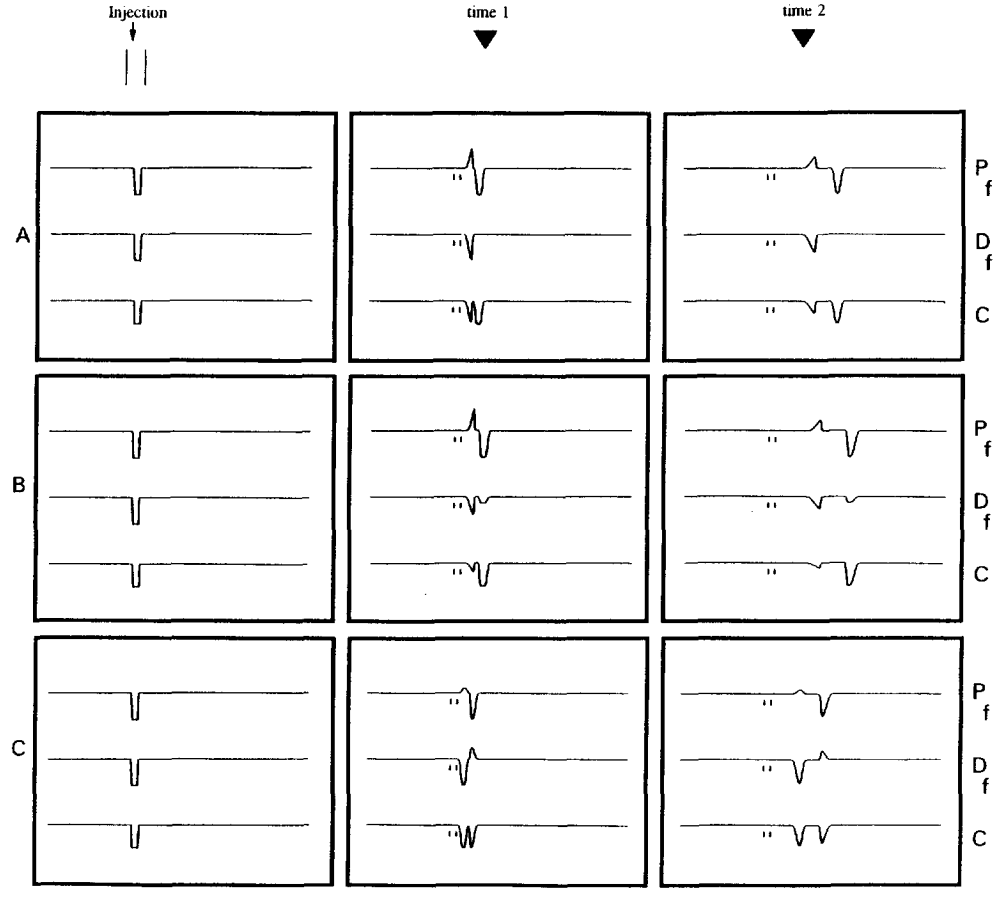

Fig. 6. Simulated concentration–position profiles for the VP (VACE) method, abscissa is position (1 and 2) in capillary. Injection marked by (| |). Assumptions: (A) $\mu_C = \mu_P > \mu_D$; (B) $\mu_C > \mu_P > \mu_D$; (C) $\mu_C < \mu_P > \mu_D$.

In the profile of P a negative as well as a small positive peak can be seen. The negative peak is representing the concentration of free P in the buffer, migrating with the mobility of free P. The positive peak in the concentration–position profile of free P is arising at the migration time of D.

The P-vacancy has a symmetric peakshape, indicating that there is no local disturbance in the concentration of the interacting species; as can be seen in Fig. 6A the concentration of free D is not disturbed in the P-vacancy.

2.6.2. Case B: $\mu_C > \mu_P > \mu_D$

The simulated concentration–position profiles are shown in Fig. 6B. In the profile of free D in case B, two negative peaks instead of one can be seen. The largest one (second peak to be detected) is representing the concentration of free D. Compared to case A, the area of this (negative) peak is decreased. This is caused by the fact that more complex is migrating into this zone before a steady state is reached. Due to the dissociation of the complex, more free D will be liberated in this zone, causing a decrease in the (negative) peak area, when compared to case A. The electropherogram, observed with e.g., UV, is a summation of all the concentration–position profiles. As a result the area "representing" the free drug concentration will be too small, and as a result the values found for the binding parameters will be too high.

The smallest negative peak (first one) in the profile of free D, migrating with the mobility of P, is caused by the fact that at the front edge of this zone complex is lacking. Free P will associate there with free D to retain the equilibrium, causing a vacancy in the local free D concentration.

In the profile of the complex two negative peaks can be seen, the largest one represents the concentration of the complex. This peak is broadened when compared to case A. This can be explained with a similar reasoning as described in Section 2.3.2. Furthermore a small negative peak arises at the migration time of D. The area of this peak is decreased when compared to case A because more complex is present in this zone as discussed.

In the profile of free P a large negative and a small positive peak can be seen. The negative peak is representing the concentration of free P in the buffer. The small positive peak, arising at the migration time of free D, is caused by the dissociation of the complex.

2.6.3. Case C: $\mu_C < \mu_P > \mu_D$

The simulated concentration–position profiles for case C are shown in Fig. 6C. In the profile of free D, a negative peak and a positive peak can be seen. The negative peak (second peak to be detected) is representing the concentration of free D. Compared to case A, the area of this (negative) peak is larger. In case C almost no complex will enter this zone, it will dissociate at the rear edge of the zone because D is lacking there. In case C the area representing the actual free D concentration in the buffer approximates the "true value" the best. However, the electropherogram, observed with e.g., UV, is a summation of all concentration–position profiles, therefore the area "representing" the free D concentration will be too large (Fig. 6C). As a result the obtained values for the binding parameters will be too low.

The positive peak (first one) in the profile of free D, migrating with the mobility of P, is caused by the fact that at the rear edge of the zone complex will dissociate because P is lacking there, and in this way also generating free D.

In the profile of the complex two negative peaks can be seen. As almost no complex is present in the D-vacancy a large negative peak can be seen migrating with the mobility of the D-vacancy (second peak to be detected). The area of this negative peak in the profile of C exceeds the area of the positive peak in the profile of free P. The second one (first one to be detected) represents the concentration of the complex in the buffer. This peak is broadened when compared to case A. This can be explained in a similar way as described in Section 2.3.2.

In the profile of free P a negative peak arises at the migration time of P. The area of this peak is decreased when compared to case A, because complex at the rear edge of this zone will dissociate because P is lacking, liberating free P and D.

The tiny positive peak arising at the migration time of the D-vacancy is caused by the dissociation of the complex that has entered this zone.

In Table 1 an overview is presented of the

deviation of the values of K_b using the VP method under the conditions chosen.

2.7. Vacancy affinity capillary electrophoresis (VACE) method

The experimental set-up of the VACE method and the VP method are identical. Apart from using the area of the negative peak in the vacancy peak method, information on the binding constant can also be attained from the shift in the migration times of the (negative) peaks. This new method is called the vacancy affinity capillary electrophoresis (VACE) method [26,27]. The mobility of the two negative peaks depends on the concentration of the component which is varied in the buffer. The situation will be described in which the concentration of D is varied and the concentration of P is kept constant.

Upon increasing the concentration of D, the mobility of the negative peaks will shift. This can be explained in the following manner: the average mobility of the peak of P (first negative peak) is determined by the fraction of free P, α, migrating with the mobility of free P, $\mu_{P,o}$, and the fraction P bound, $(1-\alpha)$, migrating with the mobility of the complex, μ_C. The average mobility of the peak of P, $\mu_{P,D}$, can be expressed as:

$$\mu_{P,D} = (1-\alpha)\mu_C + \alpha\mu_{P,o} \quad (9)$$

For the peak of D (second negative peak), the behaviour of the mobility is similar. The average mobility of the peak of D, $\mu_{D,P}$, can be expressed in the same manner:

$$\mu_{D,P} = (1-\beta)\mu_C + \beta\mu_{D,o} \quad (10)$$

where the fraction of free D in the buffer is reflected by β, migrating with the mobility of D free, $\mu_{D,o}$, and the fraction of bound D is reflected by $(1-\beta)$, migrating with the mobility of the complex, μ_C.

The VACE method relates the change in the mobility, $\mu_{P,D}$, of (bound) P and the change in the mobility, $\mu_{D,P}$, of (free) D as a function of the concentration of free D in the buffer, $[D_f]$. This relationship enables the determination of the binding constant K_b [26] and K_b for the number of binding sites, n_{bind} [27], respectively.

Because the experimental set-up of the VACE method is identical to the VP method; the described migration processes (Fig. 5a–c) and the results of the computer simulations (Fig. 6A–C) for the VP method are also valid for the VACE method. Therefore only the results of the computer simulations on the binding constant will be discussed. These are presented in Table 3.

2.7.1. Case A: $\mu_C = \mu_P > \mu_D$

When the mobility of P and the complex are equal only the shift in the mobility of D can be used to determine the binding constant. No shift in the migration time of the P-vacancy can be noticed, upon increasing the concentration of D in the buffer as $\mu_P = \mu_C$. As can be seen from Fig. 6A this peak (P-vacancy) is more or less Gaussian; indicating that in case A there is (almost) no disturbance in the local concentrations of the interacting species in the P-vacancy.

However, in case A the shift in the mobility of D can be used to determine the binding constant with the VACE method. The shift in the mobility of D is reflecting the shift in the ratio free and bound D. As discussed with the VP method, the concentration of free D in the buffer is locally, i.e., in the D-vacancy, increased due to dissociation of the complex in this vacancy. As a result the value estimated for the binding constant, K_b, using the shift in the mobility of the D-vacancy, may be too high when $\mu_P = \mu_C$. This was checked by computer simulations and turned out to be +5%, under the conditions chosen (see Table 3).

Due to the local disturbance in the concentrations

Table 3
Values for K_b obtained for the VACE method for cases A, B, C, D, E and F using computer simulations

	P-vacancy $K_b \cdot 10^{-4}$ l/mol	D-vacancy $K_b \cdot 10^{-4}$ l/mol
Case A	Impossible	1.68 (+5%)
Case B	1.58 (−1%)	4.63 (+190%)
Case C	1.44 (−10%)	1.79 (+12%)
Case D	Impossible	1.81 (+13%)
Case E	1.25 (−22%)	0.96 (−40%)
Case F	1.14 (−29%)	5.64 (+253%)

K_b theoretical: $1.60 \cdot 10^{-4}$ l/mol, $[P_{total}]$: 50 μmol/l and $[D_{total}]$: 0–2000 μmol/l.

of the interacting species the shape of this peak is asymmetric.

2.7.2. Case B: $\mu_C > \mu_P > \mu_D$

In case B the shift in the mobility of both negative peaks can be used to determine the binding constant (see Fig. 6B). As discussed with the VP method, the concentration of free D in the buffer in both zones is not equal to the free D concentration in the buffer. This disturbance in the local concentrations of the interacting species will result in a asymmetric shape of both negative peaks.

In the D-vacancy, the concentration of D is increased due to dissociation of the complex. As a result the values estimated for the binding constant, K_b, will be considerably too high: +190% under the conditions chosen (see Table 3). In case B the values are even higher than those obtained in case A, using the D-vacancy, because more complex is entering this zone before the steady state is reached.

In the P-vacancy the concentration of free D is decreased due to binding of D with free P to retain the equilibrium at the front edge of the P-vacancy. However the results obtained from computer simulations revealed that the value obtained using the P-vacancy in case B will be rather accurate: −1% under the conditions chosen (see Table 3).

In case B the P-vacancy should therefore be used to obtain a value for K_b.

2.7.3. Case C: $\mu_C < \mu_P > \mu_D$

Analogous to case B the shift in the migration time of both peaks can be used to obtain the binding constant. In this case the peak representing the D-vacancy is symmetrical (see Fig. 6C); indicating that there is almost no disturbance in the local concentration of the interacting species as already discussed with the VP method in case C. The results obtained from computer simulations revealed that the value for K_b obtained using the D-vacancy will be 12% too high under the conditions chosen (see Table 3).

In the P-vacancy the concentration of free D is increased due to dissociation of the complex to retain the equilibrium at the front edge of the P-vacancy. The value for K_b obtained from computer simulations were found to be 10% too low under the chosen conditions (see Table 3).

2.8. Frontal analysis (FA) method

In the frontal analysis method, the experimental set up is quite different. First the capillary is filled with buffer and subsequently a large sample plug is injected (Fig. 1C).

This sample plug consists of D and P in equilibrium; e.g., the concentration of D is varied and the concentration of P is kept constant. The sample plug will contain free D, free P and complex (C) [27,38–40]. A requirement for the application of the FA method is that the mobility of free D differs sufficiently from the mobility of the complex and free P. Due to the difference in mobility, free D leaks out of the plug and the height of the plateau of D is a measure of the free D concentration in the injected sample [39]. In the concentration–position profile (Fig. 1C) two plateaus will be visible, one of these plateaus is related to free P and the complex, indicated by (●), the other plateau is related to free D, indicated by (*). The height of the latter plateau is linearly related to the concentration of free D, $[D_f]$.

2.8.1. Case A: $\mu_C = \mu_P > \mu_D$

In Fig. 7a (lines 1–4) a scheme of the migration process is shown for the FA method when the mobilities of free P and complex are equal. The occurrence of the two plateaus may be explained in the following manner: After injection (line 1) all species will start migrating with their own mobilities. Part of D will be bound by P, and migrate with the mobility of C, μ_C, and part of D will migrate as free D, μ_D, as a result free D will migrate out of the zone of free P and C (line 2). As a result the average mobility of D is increased. At the front edge of the C zone the complex will dissociate (lines 3–4), because free D is lacking there. As a result, a zone of pure P develops ahead of the C-zone. At the rear edge of the free P and C zone, free P can form complex with D (lines 3–4), because free D is present here.

This situation is extremely favourable: the $[D_f]$ value is measured without any complication. As $[D_{total}]$ and $[P_{total}]$ are known, the measurement allows to calculate $[D_b]$.

2.8.2. Case B: $\mu_C > \mu_P > \mu_D$

In Fig. 7b (lines 1–4) the migration of the zones is

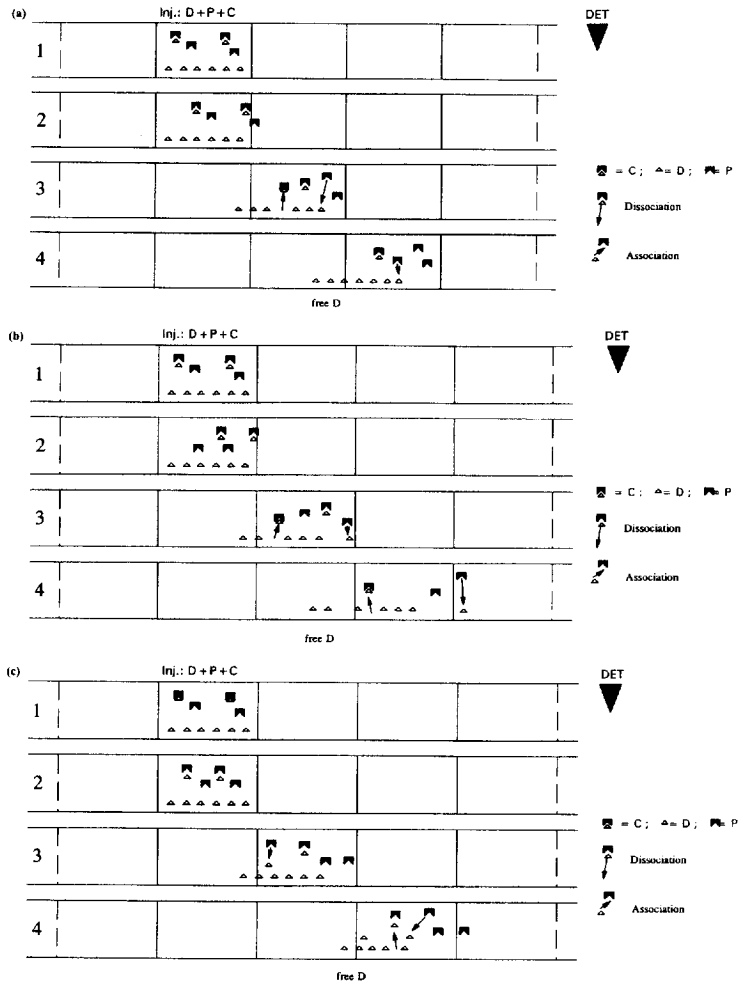

Fig. 7. (a) Illustration of the migration of the injection zone in the FA method for case A; assumption: $\mu_C = \mu_P > \mu_D$. (b) Illustration of the migration of the injection zone in the FA method for case B; assumption: $\mu_C > \mu_P > \mu_D$. (c) Illustration of the migration of the injection zone in the FA method for case C; assumption: $\mu_C < \mu_P > \mu_D$.

illustrated when the mobility of C is larger than the mobility of free P. A difference in the mobilities of free P and C will result in a decrease of the free D concentration, in the zone leaking out. This may be explained as follows: free D will be "left behind" by free P and the complex (lines 1–2) because the average mobility of free D is smaller.

As the mobility of the complex is larger than the mobility of free P, the complex will migrate ahead of the rear boundary (line 3) of the P zone, leaving a region where the equilibrium is disturbed, as free P and D are present here but no C. The resulting reaction consumes D, and its concentration in the zone leaked out is lower (line 4). The height of the plateau representing free D will be decreased. As a result, in case B the obtained values for the binding parameters will therefore be too high.

As can be seen in Fig. 7b, for this particular set of parameters, at the front edge, no pure P-zone is developing: D moves as fast as P and C. This can be understood as D "piggybacking" on P, as C (with high μ_C), overtaking free P from the rear of the zone forward.

2.8.3. Case C: $\mu_C < \mu_P > \mu_D$

In Fig. 7c (lines 1–4) the migration of the zones is

illustrated when the mobility of C is smaller than the mobility of free P. A difference in the mobilities of free P and C will result in an increase of the free D concentration, in the zone leaking out.

This may be explained as follows: since the mobility of P is larger than the mobility of the complex, P will migrate ahead of the rear boundary (line 1–3), leaving a region where the equilibrium is disturbed here because C and D are present but no P. As a result the complex will dissociate to retain the equilibrium, liberating free P as well as D there. The concentration of D in the zone leaked out is therefore higher (line 4) when compared to case A. The height of the plateau representing free D will be increased. As a result, in case C the obtained values for the binding parameters will therefore be too low.

As can be seen, for this particular set of parameters, at the front edge, also in case C a pure P-zone is developing: P moves out of the C and D zone.

As can be seen in Fig. 7c the complex and also the free D zone will be shorter, when compared to case A.

2.9. Simulated concentration–position profiles for the frontal analysis method

2.9.1. Case A: $\mu_C = \mu_P > \mu_D$

The simulated concentration–position profiles for case A are shown in Fig. 8A. As can be seen in this figure, the front edge in the profile of the complex zone coincides of course with the front edge in the profile of the free D zone; the complex can only be

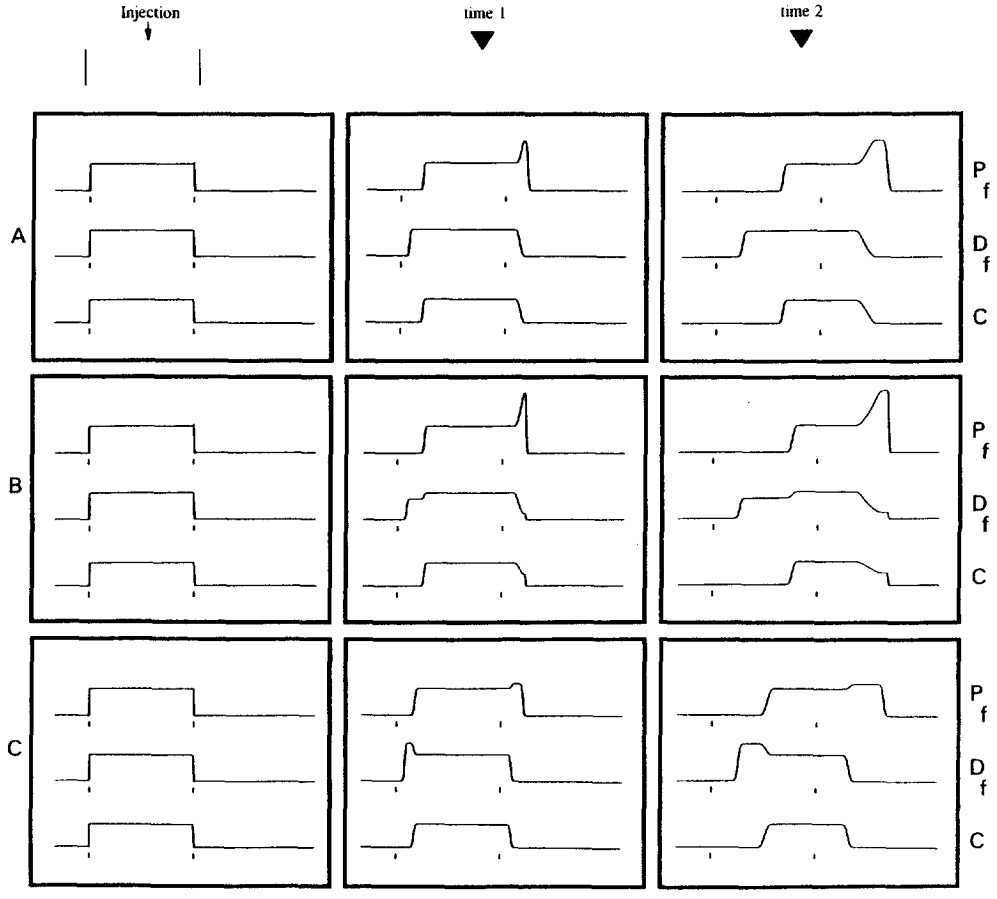

Fig. 8. Simulated concentration–position profiles for the FA method, abscissa is position (1 and 2) in capillary. Injection marked by (| |). Assumptions: (A) $\mu_C = \mu_P > \mu_D$; (B) $\mu_C > \mu_P > \mu_D$; (C) $\mu_C < \mu_P > \mu_D$.

formed when free D is present. Furthermore, it can be seen that the front edge in the profile of the free P zone exceeds the front edge of the profile of the complex zone, although the mobilities of free P and the complex are equal. This is caused by the fact that complex can only be formed when free D is present. The rear edges of the free P and the complex zone will coincide of course.

As long as the free P zone overlaps with the free D zone the complex will remain intact in the middle zone. It can be seen in Fig. 8A, that the height of the plateau of free D leaking out of the middle of the free P and C zone will reflect the correct concentration of free D in the injected sample.

2.9.2. Case B: $\mu_C > \mu_P > \mu_D$

In Fig. 8B the simulated profiles are presented for case B. Also in this case the front edges of the free D and the complex zone will coincide. After complex formation D and P will be 'moved' to the front edge of the complex zone. As a result the front edges of the free P zone and the complex zone will coincide. Due to the difference in the mobilities of free P and the complex, the zones of free P and free D will be broadened when compared to Fig. 8A. Due to this broadening of the zones the concentration of free D and free P in the zones will be decreased. In case B the height of the free D plateau will not reflect the free D concentration in the injected sample; it will be too low. As a result, in case B the obtained values for the binding parameters will be too high.

2.9.3. Case C: $\mu_C < \mu_P > \mu_D$

In Fig. 8C the simulated concentration–position profiles are presented for case C. Also in this case the front edges of the free D and the complex zone will coincide. The front edges of the free P zone and the complex zone will not coincide as P is migrating ahead of the complex.

Due to the difference in the mobilities of free P and the complex, the length of the zones of C and free D will be decreased when compared to Fig. 8A. The height of the free D plateau will not reflect the free D concentration in the injected sample; it will be too high. As a result, in case C the obtained values for the binding parameters will be too low.

In Table 1 an overview is presented of the magnitude of the deviations of the values of K_b using the FA method under the conditions chosen.

2.10. Results of the computer simulations for cases D, E and F, where $\mu_D > \mu_P$, μ_C

Cases D, E and F, for which the mobility of D is larger than the mobility of P and C were investigated also by computer simulations for the sake of completeness.

The results of cases D, E and F are shown in Fig. 9 for respectively, the HD (ACE), the VP (VACE) and the FA methods. The pictures correspond to about the same time as those in the right most column of Figs. 4, 6, and 8, respectively.

Most, if not all, of the observations that can be made in Fig. 9 are simply the mirror image of what could be observed in the simulations for cases A–C, shown in Figs. 4, 6, and 8. Also, the explanations of what can be seen can be readily derived from the reasoning applied before. Therefore we only briefly discuss Fig. 9.

2.10.1. HD, VP and FA methods

For the HD method the concentration–position profiles in Fig. 9 (first column, from top to bottom: respectively, cases D, E and F) can be compared with the concentration position profiles at position 2 (third column) in Fig. 4. For the VP method the profiles in the second column in Fig. 9 can be compared with profiles in the third column in Fig. 6. Similarly for the FA method the profiles in the third column in Fig. 9 can be compared with the profiles shown in the third column in Fig. 8.

When comparing cases A–C with D–F for the HD, the VP and the FA methods it can be noticed that the conclusions from the computer simulations for case A and D are the same. The results in case E, will be the opposite of the results found for case B, and the results found in case F will be the opposite of the results found for case C. The explanation of the results is similar to what has been mentioned in Section 2.2 Section 2.5 Section 2.8, respectively.

In Table 1 an overview of the results of is presented.

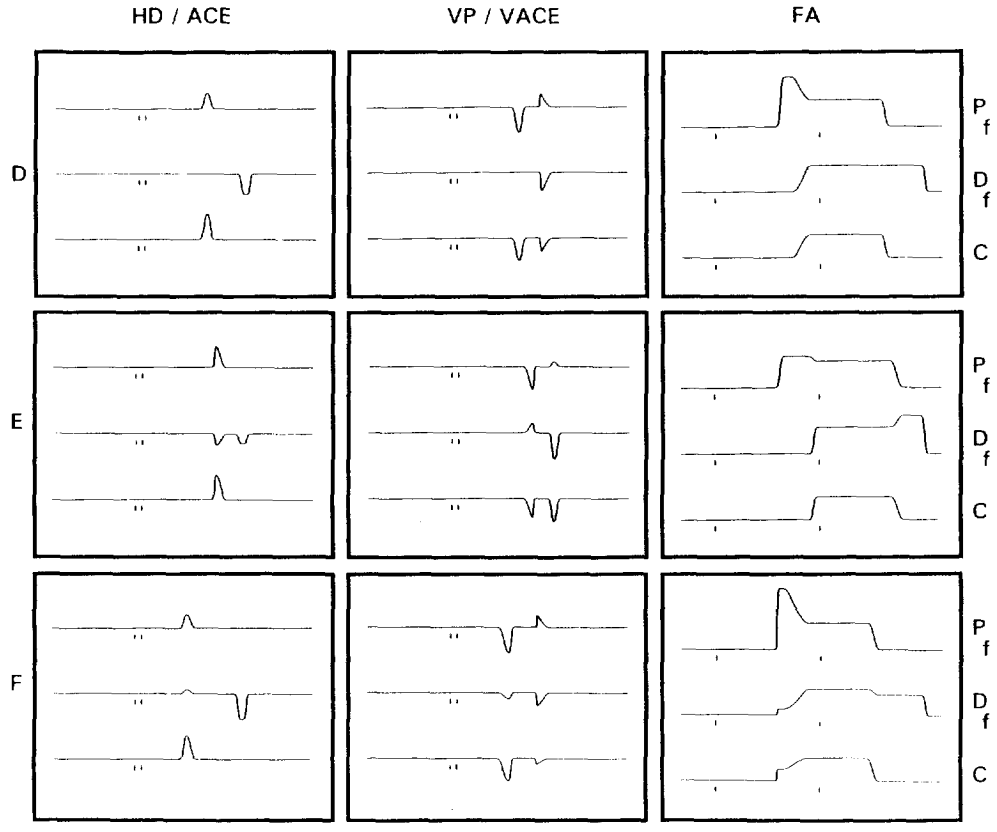

Fig. 9. Simulated concentration–position profiles for the HD (ACE), the VP (VACE) and the FA methods for cases D, E and F, abscissa is position (only 2) in capillary. Assumptions: (D) $\mu_D > \mu_C = \mu_P$; (E) $\mu_D > \mu_C > \mu_P$; (F) $\mu_D > \mu_C < \mu_P$.

2.10.1.1. HD method

With the HD method correct results for the values of the binding parameters can only be obtained in case A or D. In cases B, C, E and F it is inevitable that the outcome of the values for the binding constant will contain a systematic error. Its magnitude in cases B, C, D and F depends on the difference in the mobilities of P and C and on the concentration ratio of P and D. This error may be minimized by decreasing the concentration of P in the sample as much as possible.

2.10.1.2. VP method

As can be seen in Table 1 correct results for the values of the binding parameters can not be obtained with the VP method. In all cases it seems inevitable that the outcome of the values for the binding constant will contain a systematic error; in our opinion the area found in cases A and D approximates the "true value" for the free D concentration the best. The magnitude of the systematic error in the obtained binding parameters in cases B, C, E and F depends on the difference in the mobilities of P and C. This error may be minimized, when the concentrations in the zones deviate only little from the buffer concentrations. This can e.g., be accomplished by injecting a small plug of buffer. However, as is the case with the ACE method, detection limitations often makes this impossible.

2.10.1.3. FA method

The FA method can only be performed in cases A or D to obtain correct results for the binding constant (see also Table 1). The magnitude of the systematic error in the obtained binding parameters in cases B,

C, E and F depend on the difference in the mobilities of P and C.

2.10.2. ACE and VACE methods

As already discussed the experimental set-up of the ACE and the VACEs method are identical to the HD and the VP methods, respectively. Therefore the results of the computer simulations (Fig. 9) obtained for the HD and the VP methods also apply respectively, to the ACE and the VACE methods. Only the results of the computer simulations on the binding constant will be discussed here.

2.10.2.1. ACE method

In Table 2 an overview is presented of the values found for K_b using the ACE method with the chosen experimental conditions. These values should be seen as preliminary results of work done on this subject for the chosen conditions.

The ACE method can only be performed if the mobility of the injected P is not equal to the mobility of the complex, cases B, C, E or F. Therefore, it is inevitable that the outcome of the values for the binding constant will contain a systematic error. The magnitude of systematic error in the obtained binding parameters in cases B and C depends on the difference in the mobilities of P and C, while it can be minimized by decreasing the concentration of P in the sample as much as possible. However, in CZE the latter is often not possible because of insufficient sensitivity in the detection.

2.10.2.2. VACE method

In Table 3 values are presented for K_b using the VACE method under the conditions chosen. These values should also be seen as preliminary results of work done on this subject under the conditions chosen. Although the VACE method can be used in all cases, it is inevitable that the outcome of the values for the binding constant will contain a systematic error. The magnitude of the systematic error in the obtained binding parameters in all cases seems to depend on the difference in the mobilities of D, P and C in combination with the vacancy which is used.

This error can be minimized, when the concentrations in the zones deviate only little from the buffer concentrations. This can e.g., be accomplished by injecting a small plug of buffer. However, as is the case with the ACE method, detection limitations often makes this impossible.

2.11. Multiple equilibria

Binding studies, considering the binding of D to P, involve the determination of the binding constants. When dealing with multiple equilibria, the D–P interactions are analyzed assuming that D is bound to m classes of identical, independent binding sites. The fraction r of bound D molecules per molecule of P is often described by:

$$r = \frac{[D_b]}{[P_{total}]} = \sum_{i=1}^{m} n_i \frac{K_i[D_f]}{1 + K_i[D_f]} \quad (11)$$

where $[D_f]$, $[D_b]$ and $[P_{total}]$ are, respectively, the concentrations of free D, bound D and total P; n_i is the number of sites of class i and K_i is the corresponding binding constant [1,2].

In the case of multiple equilibria it is therefore important to be able to obtain the successive binding constants as well as the absolute numbers of the different binding sites with a certain method. A plot of r, representing the part of D that is bound by P, vs. the free D concentration, allows for the estimation of the values for the binding constants, K_i, as well as the numbers for the corresponding binding sites, n_i. As will be discussed in Section 2.11.1 below it is not possible to measure the fraction of D that has been bound by P for all the CZE methods, and consequently it is therefore not possible to obtain values for n_i using these CZE methods.

2.11.1. FA, HD and VP methods

With the FA and the VP method the concentration of free D can be determined in the sample, or in the buffer respectively, and the total concentration of P and D in the sample, or in the buffer respectively, are known. The value found for r using Eq. (11) is representing the fraction of bound molecules of D per molecule of P. With the FA and the VP method it is therefore possible to determine e.g., both binding constants, K_1 and K_2, and also the absolute numbers of the different binding sites: n_1 and n_2.

With the HD method the total concentration of P in the sample is known, and the amount of D bound

by P is measured. Furthermore the free D concentration can be set equal to the concentration of D in the buffer (also known). As a result, also with the HD method it is possible to calculate r [27].

Knowing the concentration of free D and the corresponding value for r, a binding isotherm can be constructed ($r=f[D_f]$), allowing the extraction of values for: K_1, K_2 and n_1, n_2 by considering it as a summation of Langmuir terms.

2.11.2. VACE method

With the VACE method the situation is different. In this method we are not able to measure the concentrations of the free and bound D or P in the buffer. In fact we are measuring the ratio of the fractions free and bound D, respectively free and bound P, in the buffer as a shift in the mobility of the D-vacancy respectively P-vacancy. With the VACE method both the shift in the mobility of P, $\mu_{P,D}$, and the shift in the mobility of D, $\mu_{D,P}$, can be plotted against the concentration of D in the buffer to extract the binding constant.

The latter mode ($\mu_{D,P}$ vs. $[D_{total}]$) in addition allows to estimate the number of binding sites n_i, as has been demonstrated [26,27].

When the relationship between the shift in the mobility of P, $\mu_{P,D}$ and the concentration of D in the buffer is used, on the other hand, it is only possible to obtain the binding constants K_i, but not the values for n_i. The shift in the mobility of the peak of P is representing the part of P that will be bound to D. As already discussed, to obtain information about the binding sites, we have to plot the fraction of D that has been bound by P (y-axis) versus the concentration of D in the buffer (Eq. (11)).

To obtain correct results for the binding parameters the free D concentration is the parameter that should be plotted on the x-axis. Although, it is not possible to measure the free D concentration with the VACE method, the free D concentration can be calculated. These calculations can be incorporated in the non-linear regression procedure, used to extract the binding parameters from the data. In this way the obtained binding parameters will be corrected for the difference in $[D_{total}]$ and $[D_f]$ [26,27].

2.11.3. ACE method

With the ACE method the fraction of the injected P that will form a complex with D is measured, and not the concentration of bound D in the buffer. The shift in the mobility of the peak of P is representing the part of P that has bound D. As already discussed with the other methods, to obtain values for n_i, representing the different binding sites on P, one has to plot the fraction of D that has been bound by P, vs. the concentration of free D. Therefore with the ACE method only values for K_b can be obtained and not the values for n_i [26].

2.12. Data processing for the CZE methods

2.12.1. FA, HD and VP methods

The FA, the HD and the VP methods allow the construction of the binding isotherm, as already discussed. However, a direct plot of r versus D_f (Langmuir isotherm) is not suitable for simple forms of regression to obtain values for K_i and n_i. Therefore the usual approach of binding studies is to transform Eq. (11) into a so-called Scatchard-plot [41,42]: $(r/[D_f])=f(r)$. The Scatchard plot will show a straight line when describing a 1:1 complex, whereas with multiple binding sites on P, several straight parts in the plot may be discernable. The most important limitations concerning this approach have been reviewed recently [43–47]. Kermode [47] pointed out that the application of linear regression to Scatchard data in order to calculate the binding parameters can no longer be accepted as an appropriate quantitative approach. The graphical and statistical analysis of raw, untransformed data has become an imperative in binding studies [2].

Therefore, instead of using the Scatchard plot the experimental data can be fitted according to Eq. (11), $r=f([D_f])$, for the direct representation of the experimental data. With this r–$[D_f]$ plot a non-linear regression procedure has to be used to extract the binding parameters.

Furthermore, the FA and the VP method allow the construction of a so-called $[D_f]$–$[D_{total}]$ plot because in both methods the free D concentration is measured and the total concentration of D is known. From the $[D_f]$–$[D_{total}]$ relationship the binding constants and the number of binding sites can be estimated also by using a non-linear regression procedure. Compared to an estimation using a r–$[D_f]$ (Langmuir) plot or an estimation from the commonly used Scatchard

Table 4
Comparison of the information that can be obtained with the studied CZE methods

	Monovalent complex (P:D)		Multiple equilibria e.g., ($P:D_2$)			
	k_1	n_1	k_1	n_1	k_2	n_2
FA	+	+	+	+	+	+
HD	+	+	+	+	+	+
VP	+	+	+	+	+	+
ACE	+	–	+	–	+	–
VACE ($\mu_{P,D}$) P-vacancy	+	–	+	–	+	–
VACE ($\mu_{D,P}$) D-vacancy	+	+	+	+	+	+

plot, $r/[D_f]=f(r)$, this $[D_f]$–$[D_{total}]$ relationship has the advantage that measurements errors do not affect the x-values of the plot, which gives a clearer statistical interpretation [27,40].

2.12.2. ACE and VACE method

The situation is different for the ACE and the VACE method, because with these two methods the free (or bound) concentration of D cannot be measured. Instead the shift in the mobility of the interacting species is measured. This shift is representing the ratio of the fractions free and bound D and P, respectively.

With the ACE method the free concentration of D in the zone is usually set equal to the concentration of D in the buffer. However, as was already discussed, within the P-zone, the $[D_f]$ value is different, which introduces an error.

With the VACE method the free concentration of D in the buffer has to be calculated [26]. However, analogous to what is the case with the ACE method, the concentration in the migrating zones is not always equal to the concentration of free D in the buffer.

In order to extract the binding constant a direct plot of $\mu_{P,D}$ or $\mu_{D,P}$ vs. the $[D_{buffer}]$ has the preference over the Scatchard plot in both the ACE and the VACE method.

2.12.3. Relationship between the mobilities of the interacting species: μ_P, $\mu_{P:D}$, $\mu_{P:Dn}$

When considering the ACE and the VACE method in the case of multiple equilibria, in the above mentioned data processing methods it is assumed that the mobilities of free P, the 1:1 (D:P) complex and the n:1 (D_n:P) complex are linearly related to each other. If this is not the case, this relationship between the mobilities of these $(n+1)$ species should be known and dealt with in the dataprocessing [27], inevitably complicating this, often beyond practical limits.

The relationship between the mobilities of these $(n+1)$ species is of no concern when considering the FA, the HD and the VP methods. Therefore, the FA, the HD and the VP methods have the preference when dealing with multiple equilibria in our opinion.

3. Comparison of the available CZE methods and conclusions

In Table 4 an overview is presented of the binding parameters that can be obtained with the CZE methods. As can be seen from Table 4, when dealing with a monovalent complex all methods perform equally well, because in this case it is not necessary to obtain a value for n. However, in the case of multiple equilibria, the FA, the HD, the VP and the VACE ($\mu_{D,P}$) methods have the preference because with these methods it is possible to obtain values for n_1 and n_2. However, a disadvantage of the FA, the HD and the VP methods is the fact that the mobility of the complex and free P should be almost equal to obtain correct results. This will restrict the number of applications with these methods. However as discussed with the ACE and the VACE methods, the values obtained for the binding constant with these methods will always contain a systematic error, this may be minimized. In Fig. 10 an overview is presented to guide the selection of an appropriate

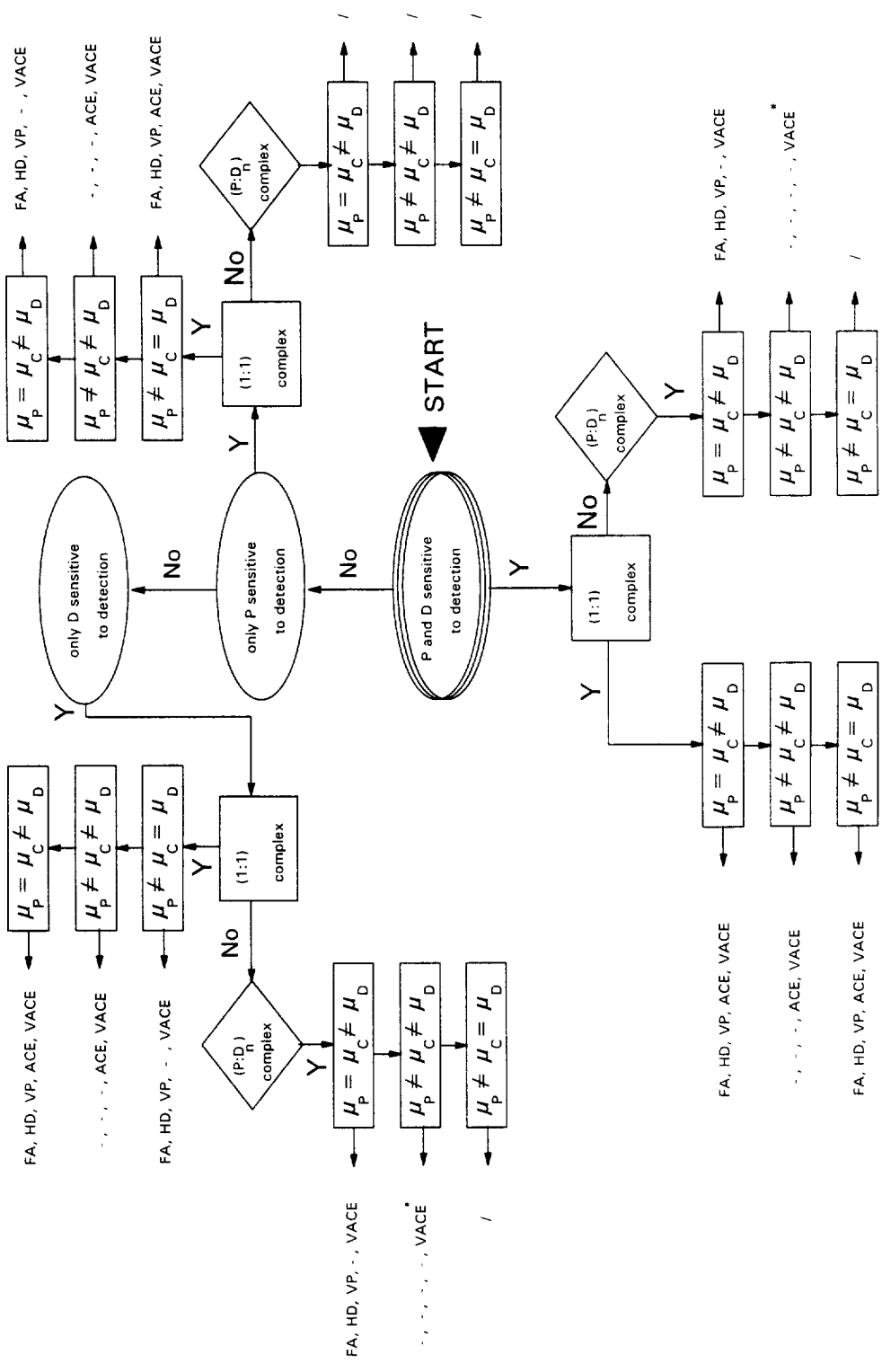

Fig. 10. Guideline for the selection of an appropriate CZE method for a certain complex system.

CZE method for a certain complexation reaction. In this overview several factors were considered: the sensitivity of D and P to the applied detection technique, the need to obtain the absolute numbers of the different binding sites in case of multiple equilibria and the mobilities of free P, free D and the complex. When all methods can be chosen the FA method has the preference because it is a simple and robust method, enabling maximum information. Furthermore this method can be performed with the smallest amount of sample when compared to the other methods. The ACE method, although also a very practical method, has a disadvantage compared to the FA method: the obtained binding constant may be systematically too high/low. In the case of a monovalent complex system and both the ACE and the VACE method can be chosen, the ACE method has the preference from the point of view of simplicity.

In the case that only the VACE ($\mu_{D,P}$) method can be used in combination with multiple equilibria, the relationship between the interacting species should be known and dealt with in the data processing step, inevitably complicating thus even further. The obtained binding parameters will otherwise be incorrect. In the overview the VACE ($\mu_{D,P}$) method is therefore marked with a "*".

Acknowledgments

The authors thank Ir. H.F.M. Boelens for his excellent technical contribution and helpful discussions. Astra Hässle, Sweden, is acknowledged for financial support.

References

[1] B. Sebille, R. Zini, C.-V. Madjar, N. Thaud, J.-P. Tillement, J. Chromatogr. 531 (1990) 51.
[2] J. Oracová, B. Böhs, W. Lindner, J. Chromatogr. B 677 (1996) 1.
[3] N.H.H. Heegaard, F.A. Robey, Am. Lab. (1991) 28T.
[4] T. Ohara, A. Shibukawa, T. Nakagawa, Anal. Chem. 67 (1995) 3520.
[5] J.C. Kraak, S. Busch, H. Poppe, J. Chromatogr. 608 (1992) 257.
[6] M.H.A. Busch, H.F.M. Boelens, J.C. Kraak, H. Poppe, J. Chromatogr. A 744 (1996) 195.
[7] Y.-H. Chu, G.M. Whitesides, J. Org. Chem. 57 (1992) 3524.
[8] F.A. Gomez, L.Z. Avilla, Y.-H. Chu, G.M. Whitesides, Anal. Chem. 66 (1994) 1785.
[9] K. Shimura, B.L. Karger, Anal. Chem. 66 (1994) 9.
[10] Y.-H. Chu, W.J. Lees, A. Stassinopoulos, C.T. Walsh, Biochemistry 33 (1994) 10616.
[11] N.H.H. Heegaard, F.A. Robey, J. Liq. Chromatogr. 16 (1993) 1923.
[12] R. Vespaleck, V. Sustacek, P. Bocek, J. Chromatogr. 638 (1993) 255.
[13] L. Valtcheva, J. Mohammad, G. Pettersson, S. Hjerten, J. Chromatogr. 638 (1993) 263.
[14] S. Busch, J.C. Kraak, H. Poppe, J. Chromatogr. 635 (1993) 119.
[15] G.E. Barker, P. Russo, R.A. Hartwick, Anal. Chem. 64 (1992) 3024.
[16] L.Z. Avilla, Y.-H. Chu, E.C. Blossey, G.M. Whitesides, J. Med. Chem. 36 (1993) 126.
[17] R. Kuhn, R. Frei, M. Christen, Anal. Biochem. 218 (1994) 131.
[18] S. Honda, A. Taga, K. Suzuki, S. Suzuki, K. Kakehi, J. Chromatogr. 597 (1992) 377.
[19] J. Liu, K.J. Volk, M.S. Lee, M. Pucci, S. Handwerger, Anal. Chem. 66 (1994) 2412.
[20] D.M. Goodall, Biochem. Soc. Trans. 21 (1993) 125.
[21] J.L Carpenter, P. Camilleri, D. Dhanak and D. Goodall, J. Chem. Soc. Chem. Commun., (1992) 804.
[22] Y.-H. Chu, L.Z. Avilla, H.A. Biebuck, G.M. Whitesides, J. Org. Chem. 58 (1992) 648.
[23] F.A. Gomez, J.N. Mirkovich, V.M. Dominguez, K.W. Liu, D.M. Macias, J. Chromatogr. A 727 (1996) 291.
[24] N.H.H. Heegaard, F.A. Robey, Anal. Chem. 64 (1993) 2479.
[25] S.A.C. Wren, R.C. Rowe, J. Chromatogr. 603 (1992) 235.
[26] M.H.A. Busch, H.F.M. Boelens, J.C. Kraak, H. Poppe, J. Chromatogr. A 775 (1997) 313.
[27] M.H.A. Busch, L.B. Carels, H.F.M. Boelens, J.C. Kraak, H. Poppe, J. Chromatogr. A 777 (1997) 311.
[28] E.V. Dose, G.A. Guiochon, Anal. Chem., 63 (1001) 1063.
[29] R.A. Moser, D.A. Saville and W. Thormann, in B.J. Radole (Editor), Electrophoresis Library; The Dynamics of Electrophoresis, VCH, Weinhein, 1992.
[30] S.V. Ermakov, M.Y. Zhukov, L. Capelli, P.G. Righetti, J. Chromatogr. A 699 (1995) 297.
[31] J.P. Hummel, W.J. Dreyer, Biochim. Biophys. Acta 63 (1962) 530.
[32] B. Sebille, N. Thaud, J.-P. Tillement, J. Chromatogr. 167 (1978) 159.
[33] D.A.Mc. Innes, L.G. Longsworth, Chem. Rev. 11 (1932) 171.
[34] F.M. Everearts, J.L Beckers and T.P.E.M. Verheggen, Isotachophoresis: Theory, Instrumentation and Applications (Journal of chromatography Library, Vol. 6), Elsevier, Amsterdam, 1976.
[35] F.A. Gomez, L.Z. Avilla, Y.-H. Chu, G.M. Whitesides, Anal. Chem. 66 (1994) 1785.

[36] M. Mammen, F.A. Gomez, G.M. Whitesides, Anal. Chem. 67 (1995) 3526.
[37] B. Sebille, N. Thaud, J.-P. Tillement, J. Chromatogr. 180 (1979) 103.
[38] J.C. Kraak, M.H.A. Busch, H. Poppe, Progress HPLC 5 (1996) 1.
[39] B. Sebille, N. Thaud, J.-P. Tillement, J. Chromatogr. 167 (1978) 159.
[40] M.H.A. Busch, H.F.M. Boelens, J.C. Kraak, H. Poppe, J. Chromatogr. A 744 (1996) 195.
[41] G. Scatchard, Ann. NY Acad. Sci. 51 (1949) 660.
[42] K.A. Conners, Binding Constants, Wiley, 1987, p. 46.
[43] L.B. Pedersen, W.E. Lindup, Biochem. Pharmacol. 47 (1994) 179.
[44] I.M. Klotz, Science 217 (1982) 1247.
[45] I.M. Klotz, Science 220 (1983) 981.
[46] K. Zierler, Trends Biochem. Sci. 14 (1989) 314.
[47] J.C. Kermode, Biochem. Pharmacol. 38 (1989) 2953.